

Kinetics of Disproportionation and  $pK_a$  of Bromous Acid<sup>1</sup>Roberto de Barros Faria,<sup>†</sup> Irving R. Epstein,<sup>\*</sup> and Kenneth Kustin<sup>\*</sup>

Department of Chemistry, Brandeis University, Box 9110 Waltham, Massachusetts 02254-9110

Received: September 14, 1993; In Final Form: November 22, 1993<sup>⊙</sup>

The kinetics of the disproportionation reaction of bromine(III),  $2\text{Br(III)} \rightarrow \text{Br(I)} + \text{Br(V)}$ , was studied in phosphate buffer, in the pH range 5.9–8.0, by monitoring optical absorbance at 294 nm using stopped-flow. The dependences on  $a_{\text{H}^+}$  and  $[\text{Br(III)}]$  were of order 1 and 2, respectively, and no dependence on  $[\text{Br}^-]$  was found. The reaction was also studied in acetate buffer, in the pH range 3.9–5.6. Within experimental error, no evidence was found for a direct reaction between two  $\text{BrO}_2^-$  ions. This study yields rate constants  $39.1 \pm 2.6 \text{ M}^{-1} \text{ s}^{-1}$  for the reaction  $\text{HBrO}_2 + \text{BrO}_2^- \rightarrow \text{HOBr} + \text{BrO}_3^-$  and  $800 \pm 100 \text{ M}^{-1} \text{ s}^{-1}$  for the reaction  $2\text{HBrO}_2 \rightarrow \text{HOBr} + \text{BrO}_3^- + \text{H}^+$  and an equilibrium quotient for  $\text{HBrO}_2 \rightleftharpoons \text{H}^+ + \text{BrO}_2^-$  of  $3.7 \pm 0.9 \times 10^{-4} \text{ M}$  ( $pK_a = 3.43$ ) at ionic strength 0.06 M and  $25.0 \pm 0.1 \text{ }^\circ\text{C}$ . The bromous acid dissociation constant is essentially identical to the value previously obtained from a kinetics study of the bromine(III)–I<sup>-</sup> reaction (*J. Phys. Chem.* 1992, 96, 6861).

## Introduction

The first relatively unambiguous determination of the  $pK_a$  of bromous acid was achieved by studying the kinetics of the reaction between bromine(III) and iodide ion.<sup>2</sup> Because this value differed significantly from some earlier estimates, we have sought other reactions of bromine(III) that could be used for the same purpose. The disproportionation of bromine(III),  $2\text{Br(III)} \rightarrow \text{Br(I)} + \text{Br(V)}$ , is such a reaction. Its kinetics can provide a second measurement of the  $pK_a$  of  $\text{HBrO}_2$ , which affords comparison of this value with the previously determined value.

We report here measurements of the rate law for the kinetics of disproportionation of bromine(III) at pH 3.5–8.0 and suggest a mechanism for this reaction. Qualitatively, the results agree with earlier studies of bromine(III) decomposition at pH 6.2–8.5, except that we find no  $[\text{Br}^-]$ -dependence.<sup>3,4</sup> From our results at pH 3.5–5.6, we present a new measurement of the  $pK_a$  of  $\text{HBrO}_2$  that confirms our previously reported value.

## Experimental Section

**Materials.** All reagents ( $\text{NaClO}_4$ , Aldrich; all the rest, Fisher) were of the highest purity available and were used without further purification, except for  $\text{NaBrO}_2 \cdot 3\text{H}_2\text{O}$  (Aldrich, no longer available), which was purified to reduce the bromide content following a procedure described elsewhere.<sup>5</sup>

**Methods.** Bromite stock solution titer was checked every week,<sup>6</sup> and the stock solution was discarded after 1 month even if its concentration was not observed to have changed.

An HP 8452A spectrophotometer was used to determine the molar absorbance of  $\text{BrO}_2^-$  in 0.01 M NaOH. An Orion 801A research pH meter, together with a combined pH electrode (Aldrich, Model Z11323-9), was used to determine pH.

Reactions were carried out in 0.05 M phosphate buffer at ionic strength  $\mu = 0.15 \text{ M}$  or in 0.05 M acetate buffer at  $\mu = 0.06 \text{ M}$ ;  $\text{NaClO}_4$  was used to adjust the ionic strength. In calculating ionic strengths, the concentrations of the ions generated by buffer and reagents were taken into consideration.

Spectra and some of the kinetics curves were determined with the HP 8452A spectrophotometer at  $25.0 \pm 0.1 \text{ }^\circ\text{C}$  using a 1-cm path quartz cuvette having a magnetic stirrer inside. A Finnpiette Digital with 1–5-mL capacity (Lab Systems) gave fast

delivery of the buffer solution into the bromite solution in the cuvette. For experiments under argon atmosphere, we bubbled the inert gas through the reagents. After mixing the reagents in the cuvette, we kept the inert gas bubbling through the surface of the reagent mixture while keeping the cuvette partially closed with Parafilm.

More precise kinetics curves were determined by monitoring absorbance at 294 nm at  $25 \pm 0.1 \text{ }^\circ\text{C}$  with a Hi-Tech SF-3L stopped-flow spectrophotometer equipped with an Orion 6316 deuterium lamp.

The method we used for the determination of the initial velocity in the acid pH range using acetate buffer was the same as previously employed, i.e., fitting a quadratic polynomial to the initial part of the kinetics curve and taking the coefficient of the linear term as the initial velocity.<sup>2</sup>

Calculations for parameter estimations used Minsq (Micro-Math Scientific Software) or SlideWritePlus (Advanced Graphics Software, Inc.), which employ least squares minimization procedures based on modifications of the Levenberg–Marquardt technique to solve linear and nonlinear problems of parameter estimation and curve fitting.<sup>7</sup>

## Results

**Phosphate Buffer.** A determination of the initial velocity of the bromine(III) disproportionation reaction in this medium is not straightforward. The initial part of the kinetics curve has a complex profile, displaying an induction period followed by autocatalytic behavior (Figure 1). Although the brief induction period must have some chemical meaning, we decided to ignore it when making our initial velocity measurements, and we analyzed the experimental data points following conversion to an absorbance scale after this initial lag period. Since oxygen has been reported to influence the kinetics of bromite reactions with other inorganic species, we obtained kinetics curves with and without argon gas as described above.<sup>8</sup> No effect was noted, and we did not pursue further use of the inert atmosphere method of kinetics data collection.

In the pH range 5.9–7.2, the logarithm of the absorbance at 294 nm varies linearly with time for several half-lives but then begins to deviate from linearity. Because of this effect, we chose to measure the initial velocity, fitting a straight line to the initial absorbances. Assuming that, in the disproportionation reaction, 2 mol of bromine(III) reacts to form products, we define the initial velocity,  $V_0$ , as follows, where  $[\text{Br(III)}]$  is total bromine(III)

<sup>†</sup> Departamento de Química Inorgânica, Instituto de Química, Universidade Federal do Rio de Janeiro, 21945-970, Caixa Postal 68563, Rio de Janeiro, RJ, Brazil.

<sup>⊙</sup> Abstract published in *Advance ACS Abstracts*, January 1, 1994.

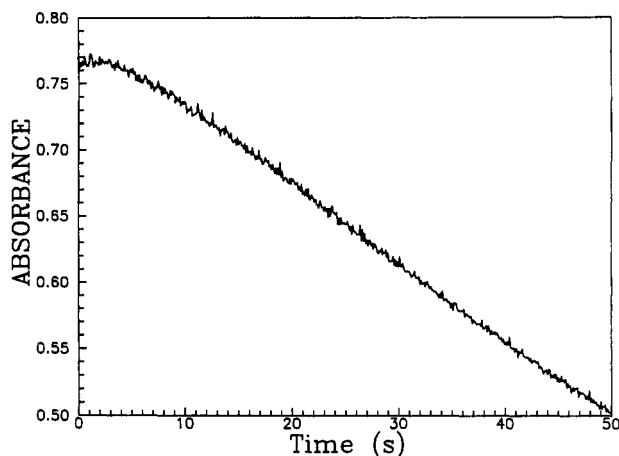


**Figure 1.** Typical trace for stopped-flow experiment at 294-nm wavelength.  $[\text{Br(III)}]_0 = 6.94 \times 10^{-3} \text{ M}$ ,  $\mu = 0.15 \text{ M}$ , 0.05 M phosphate buffer pH 5.9, average of seven kinetics curves. To show the induction period, the earliest portion of the trace is emphasized. Later portions of the trace would exhibit autocatalysis more clearly.

**TABLE 1: Stopped-Flow Results for Determination of Order with Respect to  $[\text{Br(III)}]_0$ : 0.05 M Phosphate Buffer, pH 5.9,  $\mu = 0.15 \text{ M}$  (Figure 2)**

$[\text{Br(III)}]_0$	$-dA/dt$	$-1/2(dA/dt)/\epsilon$	$\log(V_0)$
$5 \times 10^{-3}$	$2.785 \times 10^{-3}$	$1.246 \times 10^{-5}$	-4.9046
$4 \times 10^{-3}$	$1.886 \times 10^{-3}$	$8.435 \times 10^{-6}$	-5.0739
$3 \times 10^{-3}$	$1.041 \times 10^{-3}$	$4.656 \times 10^{-6}$	-5.3320
$2 \times 10^{-3}$	$4.874 \times 10^{-4}$	$2.180 \times 10^{-6}$	-5.6616

**TABLE 2: Determination of Order with Respect to  $a_{\text{H}^+}$ : 0.05 M Phosphate Buffer,  $[\text{Br(III)}]_0 = 6.94 \times 10^{-3} \text{ M}$ ,  $\mu = 0.15 \text{ M}$  (Figure 3)**

pH	$-dA/dt$	$-1/2(dA/dt)/\epsilon$	$\log(V_0)$
5.866	$6.088 \times 10^{-3}$	$2.723 \times 10^{-5}$	-4.5650
6.256	$2.656 \times 10^{-3}$	$1.188 \times 10^{-5}$	-4.9252
6.709	$7.947 \times 10^{-4}$	$3.554 \times 10^{-6}$	-5.4493
7.188	$1.800 \times 10^{-4}$	$8.050 \times 10^{-7}$	-6.0942

concentration, *i.e.*,  $[\text{Br(III)}] = [\text{HBrO}_2] + [\text{BrO}_2^-]$ :

$$V_0 = -\frac{1}{2} \left. \frac{d[\text{Br(III)}]}{dt} \right]_{t=0} \quad (1)$$

For phosphate buffer  $V_0 = -1/2(dA/dt)/\epsilon$ , where  $A_0$  is the absorbance at 294 nm at time zero and  $\epsilon$  is the apparent molar absorbance coefficient. For this buffer, to a very good approximation,  $\epsilon$  is the absorbance coefficient of bromite ion at this wavelength, equal to  $111.8 \text{ M}^{-1} \text{ cm}^{-1}$ , in good agreement with other determinations.<sup>9,10</sup>

A plot of the logarithm of initial velocity against  $\log([\text{Br(III)}]_0)$  yields a straight line with slope  $1.92 \pm 0.03$  (Table 1), where  $[\text{Br(III)}]_0$  is the total initial bromine(III) concentration. This result suggests second-order dependence on initial bromine(III) concentration.

A plot of logarithm of initial velocity against the negative of the initial pH yields a straight line with slope  $1.16 \pm 0.06$  (Table 2), implying a first-order dependence on  $a_{\text{H}^+}$ .

Addition of bromide does not accelerate the decomposition of bromite (Figure 2). When  $[\text{Br}^-]_0$  is close to  $[\text{Br(III)}]_0$ , there was an initial increase of the absorbance at 294 nm followed by a decrease after some time (Figure 2, curve c). When  $[\text{Br}^-]_0$  is in large excess over  $[\text{Br(III)}]_0$ , no further delay in absorbance was noted (Figure 2, curve d). These results suggest that the apparent induction period (e.g., Figure 1) may result from absorbance due to the products of bromine(III) disproportionation.

When the kinetics of bromine(III) disappearance was followed by acquiring a full spectrum at fixed time intervals (conditions as in Figure 2c), we observed that two bands were forming at 266

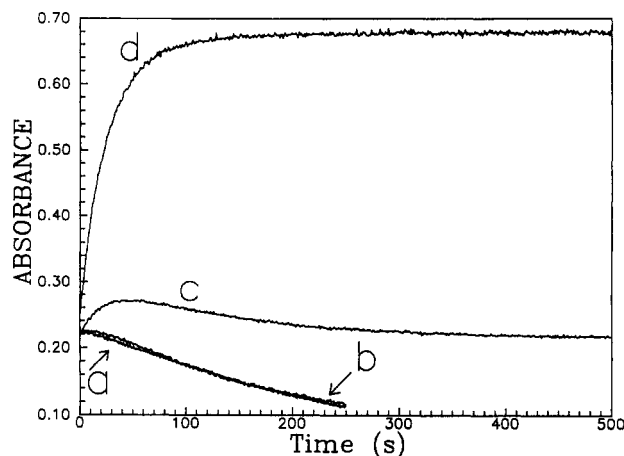


**Figure 2.** Effect of bromide addition on the kinetics curves at 294 nm.  $[\text{Br(III)}]_0 = 2 \times 10^{-3} \text{ M}$ , 0.05 M phosphate buffer, pH 5.9,  $\mu = 0.15 \text{ M}$ : (a)  $[\text{Br}^-]_0 = 2.5 \times 10^{-4} \text{ M}$ , (b)  $[\text{Br}^-]_0 = 1 \times 10^{-3} \text{ M}$ , (c)  $[\text{Br}^-]_0 = 2.5 \times 10^{-3} \text{ M}$ , (d)  $[\text{Br}^-]_0 = 5 \times 10^{-3} \text{ M}$ .

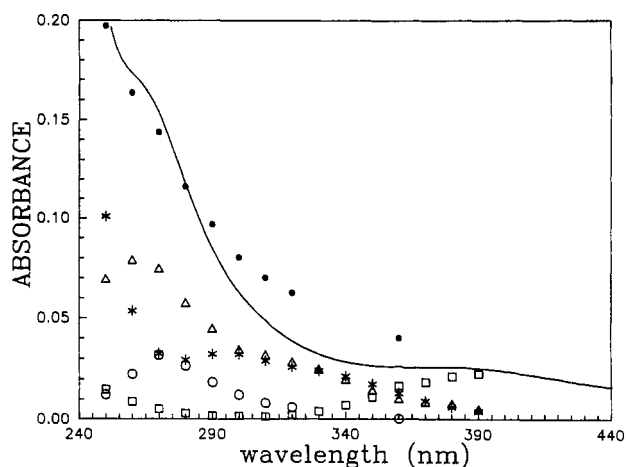


**Figure 3.** Final spectrum (after 15 min) for the disproportionation of  $5 \times 10^{-3} \text{ M}$   $[\text{Br(III)}]_0$  in phosphate buffer, pH 5.9. Attributions for the probable components calculated by a least squares procedure: (—) experimental spectrum, (●) sum of all calculated absorbances, (\*) absorbance for  $[\text{BrO}_2^-] = 2.77 \times 10^{-4} \text{ M}$ , (Δ) absorbance for  $[\text{HOBr}] = 8.58 \times 10^{-4} \text{ M}$ , (□) absorbance for  $[\text{Br}_2] = 1.27 \times 10^{-4} \text{ M}$ , (○) absorbance for  $[\text{Br}_3^-] = 8.145 \times 10^{-7} \text{ M}$ .

and 384 nm, the latter with lower intensity, at the same time that the superimposed bromite spectra were decreasing in intensity. We assigned the 266-nm band to  $\text{Br}_3^-$ , which has a maximum absorbance at this wavelength with relatively high molar absorbance ( $\epsilon \approx 3.5 \times 10^4 \text{ M}^{-1} \text{ cm}^{-1}$ ).<sup>11-14</sup>

Hydrobromous acid, HOBr, shows one maximum in its spectrum, at 260 nm, with molar absorbance  $95 \text{ M}^{-1} \text{ cm}^{-1}$ . Its molar absorbance at 294 nm is only  $50 \text{ M}^{-1} \text{ cm}^{-1}$  compared with  $\epsilon \approx 2 \times 10^4 \text{ M}^{-1} \text{ cm}^{-1}$  for  $\text{Br}_3^-$  at 294 nm. These data are consistent with attribution of the strong band appearing at 266 nm to  $\text{Br}_3^-$ . This assignment does not allow us to neglect the formation of HOBr, because its spectrum can be obscured by  $\text{Br}_3^-$ .<sup>13,15,16</sup>

We analyzed at the final stages of reaction the spectrum of a reaction mixture without any initially added bromine (Figure 3). There is a shoulder close to 266 nm and a broad band with low intensity around 380 nm. Using Minsq and molar coefficients of absorbance for  $\text{BrO}_2^-$  determined in this study and those gathered from the literature for HOBr,  $\text{Br}_2$ , and  $\text{Br}_3^-$ , we could calculate, using nine data points, the probable composition of the final reaction mixture (Figure 3).<sup>11,13</sup> Although the sum of the calculated absorbances fits the experimental result reasonably well, the best agreement is found for wavelengths no greater than 290 nm. We therefore conclude that after elapse of a fairly long reaction time some HOBr,  $\text{Br}_2$ ,  $\text{Br}_3^-$ , and even  $\text{BrO}_2^-$  are present.

TABLE 3: Molar Absorbances

wavelength (nm)	BrO <sub>2</sub> <sup>-</sup> (M <sup>-1</sup> cm <sup>-1</sup> ) <sup>a</sup>	HBrO <sub>2</sub> (M <sup>-1</sup> cm <sup>-1</sup> ) <sup>b</sup>
260		225
280	100.2	119
282	101.7	
284	103.6	103 <sup>c</sup>
286	105.7	
288	107.9	
290	109.7	
292	111.1	
294	111.8	68 <sup>c</sup>
296	112.1	
298	111.6	
300	110.5	53
330		21

<sup>a</sup> This work. <sup>b</sup> Reference 17. <sup>c</sup> Estimated in this work by using a cubic spline fitting for the data of ref 17 applied to HBrO<sub>2</sub>.

Since HOBr is a product of the disproportionation reaction, and would be expected to be an intermediate in any other mode of bromine(III) decomposition, we attempted to follow the reaction with the HP 8452A simultaneously at up to six wavelengths for which the molar absorbances of BrO<sub>2</sub><sup>-</sup> and HOBr are known. We calculated [BrO<sub>2</sub><sup>-</sup>] from a two-equation model, using the data from two different wavelengths. Although the log [BrO<sub>2</sub><sup>-</sup>] against time data showed much more linear behavior than the simple logarithm of absorbance at 294 nm, the pseudoinduction period remained. Additional attempts using three- or four-equation models to calculate [BrO<sub>2</sub><sup>-</sup>], and taking into consideration the concentrations of HOBr, Br<sub>2</sub> and Br<sub>3</sub><sup>-</sup>, were unsuccessful, because negative values for at least one concentration were calculated for the initial part of the kinetics curve. Therefore, the induction period shown in Figure 1 cannot be explained by considering only the absorbances of reaction products such as HOBr and Br<sub>3</sub><sup>-</sup>.

**Acetate Buffer.** To measure the pK<sub>a</sub> of HBrO<sub>2</sub> using its disproportionation reaction, we determined the kinetics of this reaction at different pHs in the range 3.68–5.64 using the stopped-flow method. No pseudoinduction period was observed on the time scale of these experiments, and no special problems occurred to complicate a determination of the initial velocity.

At or above pH 5, plots of logarithm of absorbance at 294 nm against time were linear for the least two or three initial half-lives. For pH 4 or lower this was not the case. A plot of the inverse of absorbance against time shows more linear behavior, suggesting that at more acidic pH values the reaction begins to show second-order behavior.

These observations can be explained by a mechanism based on only three elementary steps:



If we assume that reaction E1 is a rapid equilibrium, we obtain eq 2 for the rate of disproportionation in terms of [Br(III)], where K<sub>a</sub> is the equilibrium quotient for HBrO<sub>2</sub> dissociation and k<sub>1</sub> and k<sub>2</sub> are rate constants for reactions R1 and R2, respectively.

$$-\frac{1}{2} \frac{d[\text{Br(III)}]}{dt} = \frac{(k_1 K_a [\text{H}^+] + k_2 [\text{H}^+]^2) [\text{Br(III)}]^2}{(K_a + [\text{H}^+])^2} \quad (2)$$

As acidity increases [HBrO<sub>2</sub>] increases, and the initial spectra of the reaction mixtures must include some contribution from HBrO<sub>2</sub>. Fitting the known data for the molar absorbance of HBrO<sub>2</sub> with a cubic spline routine allowed us to estimate by interpolation a value of 68 M<sup>-1</sup> cm<sup>-1</sup> for the molar absorbance of HBrO<sub>2</sub> at 294 nm (Table 3).<sup>17</sup>

TABLE 4: Initial Variation of Absorbance as a Function of pH: 0.05 M Acetate Buffer, [Br(III)]<sub>0</sub> = 5 × 10<sup>-4</sup> M

[H <sup>+</sup> ] (M)	-dA/dt
2.698 × 10 <sup>-6</sup>	3.0476 × 10 <sup>-5</sup>
1.125 × 10 <sup>-5</sup>	2.1502 × 10 <sup>-4</sup>
4.179 × 10 <sup>-5</sup>	1.5792 × 10 <sup>-3</sup>
1.233 × 10 <sup>-4</sup>	5.8181 × 10 <sup>-3</sup>
2.000 × 10 <sup>-4</sup>	8.4001 × 10 <sup>-3</sup>
3.098 × 10 <sup>-4</sup>	1.0773 × 10 <sup>-2</sup>

Using molar absorbance data that we determined in separate experiments, and fitting the known data for the molar absorbance of HBrO<sub>2</sub> with a cubic spline routine, we estimated the isosbestic point of HBrO<sub>2</sub> and BrO<sub>2</sub><sup>-</sup> to occur at 284 nm with a common molar absorbance of 103 M<sup>-1</sup> cm<sup>-1</sup> (Table 3).<sup>17</sup>

Close to the initial reaction time, the absorbances of products should not interfere with the measured absorbance A<sub>t</sub>, and eq 3 should hold.

$$A_t = \epsilon_{(\text{HBrO}_2)} [\text{HBrO}_2] + \epsilon_{(\text{BrO}_2^-)} [\text{BrO}_2^-] \quad (3)$$

The absorbance A<sub>t</sub> is expressed as a function of [Br(III)] in eq 4.

$$A_t = \frac{[\text{Br(III)}]}{K_a + [\text{H}^+]} (\epsilon_{(\text{HBrO}_2)} [\text{H}^+] + \epsilon_{(\text{BrO}_2^-)} K_a) \quad (4)$$

Taking the derivative of [Br(III)] from eq 4 and equating it with the right-hand side of eq 2, we obtain eq 5 for initial velocity in acetate buffer.

$$v_0 = -\frac{1}{2} \left. \frac{dA}{dt} \right|_{t=0} = \frac{(k_2 \epsilon_{(\text{HBrO}_2)} [\text{H}^+]^3 + (k_1 K_a \epsilon_{(\text{HBrO}_2)} + k_2 K_a \epsilon_{(\text{BrO}_2^-)}) [\text{H}^+]^2 + k_1 K_a^2 \epsilon_{(\text{BrO}_2^-)} [\text{H}^+]) [\text{Br(III)}]_0^2}{(K_a + [\text{H}^+])^3} \quad (5)$$

Measurements of the derivative of absorbance at initial time for different pH values should allow us to determine the coefficients of eq 5 by curve fitting. Taking 68 and 111.8 M<sup>-1</sup> cm<sup>-1</sup> for the molar absorbances at 294 nm of HBrO<sub>2</sub> and BrO<sub>2</sub><sup>-</sup>, respectively, and knowing [Br(III)]<sub>0</sub>, we should be able to fit eq 5 for the best values of k<sub>1</sub>, k<sub>2</sub>, and K<sub>a</sub>. In this treatment, to convert readings of hydrogen ion activity to [H<sup>+</sup>], we use activity coefficient 0.84905 for μ = 0.06 M.<sup>18</sup>

However, finding three coefficients of eq 5 from six data points (Table 4) by use of nonlinear least squares curve fitting leaves only three degrees of freedom, too few for a statistically meaningful fit. Therefore, the following procedure was adopted. The values of K<sub>a</sub> and k<sub>2</sub> were held constant, and the value of k<sub>1</sub> and its associated Student's *t*-value were obtained by a Levenberg-Marquardt nonlinear curve-fitting procedure (SlideWritePlus).<sup>7</sup> This process was repeated for different combinations of K<sub>a</sub> and k<sub>2</sub>. The fit was most sensitive to the value of K<sub>a</sub> chosen; outside the range 2.5–5 × 10<sup>-4</sup> M, Student's *t*-value was less than 2, indicating a statistically meaningless fit. The process was repeated holding k<sub>1</sub> and k<sub>2</sub> constant and finding K<sub>a</sub>. In this case, the iterative algorithm converged on the same values of K<sub>a</sub> associated with meaningful Student's *t*-values in the fixed K<sub>a</sub> and k<sub>2</sub> trials. The set of three coefficients and their relative errors yielding a maximum in Student's *t*-value (15.01) found by this procedure are K<sub>a</sub> = 3.7 ± 0.9 × 10<sup>-4</sup> M, k<sub>1</sub> = 39.1 ± 2.6 M<sup>-1</sup> s<sup>-1</sup>, and k<sub>2</sub> = 800 ± 100 M<sup>-1</sup> s<sup>-1</sup>. The graph of V<sub>0</sub> against [H<sup>+</sup>] calculated according to eq 5 compares favorably with a plot of experimental values (Figure 4).

## Discussion

In alkaline media, our results are consistent with observations of Engel, Oplatka, and Perlmutter-Hayman<sup>3</sup> and Lee and Lister,<sup>10</sup> but not with those of Massagli, Indelli, and Pergola.<sup>4</sup> In the range pH 7–13, the earlier findings are principally as follows:

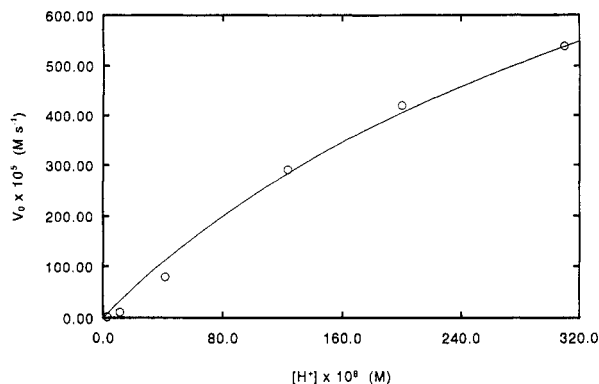


**Figure 4.** Hydrogen ion dependence of initial velocity of bromine(III) disproportionation,  $(-1/2)dA_0/dt$ , at 294 nm, 0.05 M acetate buffer,  $[Br(III)]_0 = 5 \times 10^{-4}$  M: (O) experimental values, (—) calculated curve (eq 5).

the rate of bromite disproportionation is independent of ionic strength;<sup>3</sup> it is inversely pH dependent, pH 8.5–12;<sup>3</sup> and it levels off above pH 12.<sup>10</sup> These results can be explained by our mechanism. Within experimental error, lack of an ionic strength dependence rules out a  $BrO_2^- + BrO_2^-$  reaction. Decline in  $[HBrO_2]$  with increasing pH explains the inverse pH dependence. Leveling off of rate as very high pH values are approached signifies the beginning of a shift from exclusive rate control by the  $HBrO_2 + BrO_2^-$  reaction to rate control shared between this reaction and autoprotolysis. That is, at these highly alkaline pHs, formation of  $HBrO_2$  from  $BrO_2^-$  begins to be controlled by the availability of  $H^+$  which is, in turn, controlled by the rate of dissociation of  $H_2O$ .

We found a reaction order for  $a_{H^+}$  of 1.16 in the pH range 5.9–7.2, using phosphate buffer. Massagli *et al.* found order 0.9 in the pH range 3.56–6.26 using spectrophotometric and stopped-flow techniques and order 1.16 in excess bromide.<sup>4</sup> In addition, Massagli *et al.* found order 1.87 in the pH range 6.26–8.55 using both polarographic and spectrophotometric techniques. Although we did not make precise stopped-flow experiments in a pH range as high as 8.5, we acquired some kinetics curves, using the HP8452A spectrophotometer, up to a maximum pH of 8. The kinetics remained first-order in  $a_{H^+}$ . This result suggests that the high value found by Massagli *et al.* for the order with respect to  $a_{H^+}$  in the high pH range is an artifact of the experimental technique used by these investigators in this pH range.

Our value of 1.92 at pH 5.9 suggests that the bromine(III) reaction order is 2. Using the polarographic/spectrophotometric technique, Massagli *et al.* found 1.75 at pH 7.09 and 0.92 in the presence of excess  $[Br^-]$  at the same pH. We did not observe a bromide effect on the rate of disproportionation of bromine(III), however, and our result for the bromine(III) order in the presence or absence of bromide is the same. To explain our disagreement with Massagli *et al.*, we suggest that the polarographic method is responsible.

The pseudoinduction period appears to be a real effect. A similar effect was noted by Engel *et al.* (see Figure 7 in the original paper),<sup>3</sup> and our observations agree very well with those of these authors. For example, in a preliminary set of experiments using the HP8452A spectrophotometer, we noticed that decreasing  $[Br(III)]_0$  increases this lag period and increasing  $[Br^-]_0$  increases it. This effect can be explained by formation of  $Br_2$  and  $Br_3^-$ , which make a significant contribution to the absorbance at 294 nm. As bromine(III) decomposes, it forms HOBr, which decomposes or reacts with bromite, forming some  $Br^-$ . Moreover,  $Br^-$  and HOBr can react to form  $Br_2$  which, in the presence of  $Br^-$ , forms  $Br_3^-$ . As  $Br_3^-$  increases, the absorbance at 294 nm may stay constant for a period of time or may even increase if  $[Br^-]_0$  is high enough. It is surprising, however, that this lag period was noted by Engel *et al.* during measurements of  $[Br(III)]$  in the reaction mixture by titration.

Identification of bromine as one of the final products of the decomposition of bromine(III) at near neutral pH in the presence of excess  $Br^-$  is very clear from the appearance of a strong absorption band centered at 266 nm and one additional weak band centered at 384 nm.<sup>11–14</sup> Starting from a bromine(III) solution without bromide, the final spectra suggest the presence of  $Br_3^-$ ,  $Br_2$ , HOBr, and even  $BrO_2^-$ , but agreement between the experimental and calculated spectra is not perfect. As we were unable to find data for the molar absorbance of  $Br_3^-$  at other wavelengths beyond the maximum in tabular form, we were compelled to obtain these data by estimating from the figures found in the cited papers; errors in this procedure are high. Molar absorbance data for  $Br_2$  and HOBr are in a similar condition. Summation of all these errors can explain differences between measured and calculated spectra (Figure 3). Inaccurate molar absorbances may also account for the negative values calculated for the concentrations of these species in kinetics curves obtained at more than two wavelengths. The lack of relevant molar absorbance data prevents us from ascertaining the presence or absence of additional compounds in the final reaction mixtures.

The bromous acid  $pK_a$  of  $3.43 \pm 0.9 \times 10^{-4}$  M that emerges from this kinetics study of bromine(III) disproportionation is essentially identical with the value measured from the kinetics of the reaction between bromine(III) and iodide at the same ionic strength (0.06 M).<sup>2</sup> Both methods have drawbacks, however. For example, the bromine(III)–I<sup>-</sup> reaction becomes so rapid at low pH that it encroaches on the stopped-flow resolution time, which may lead to errors in measurements of the initial velocities. It is easier to follow the disproportionation of bromine(III), because it is slower. However, products formed by the decomposition of bromine(III), e.g., HOBr,  $Br_2$ , and  $Br_3^-$ , absorb UV light in the same region used to follow this reaction. Our inability to subtract these additional absorbances from our experimental data introduces some error into our results. These errors cannot be very large, because we are measuring initial velocities, and at the start of the reaction the concentrations (and, of course, the absorbances) of the products must be small.

Phosphate buffer kinetics studies suffer from numerous experimental problems described above, such as an unaccountable induction period. Furthermore, an interaction between phosphate and some form of bromine(III) was noted while studying bromine(III)–iodide reactions.<sup>2,5</sup> Because of these problems, we do not rely on the rate and equilibrium constants determined from kinetics studies with this buffer. (There is no indication of general acid catalysis, because a change in buffer concentration does not change reaction rate, provided  $[H^+]$  is unchanged.) Two kinetics studies of the bromous acid disproportionation reaction in sulfuric acid media (0.1–2.0 M  $H_2SO_4$ ) yield apparent rate constants in the range  $1-4 \times 10^3$   $M^{-1} s^{-1}$ .<sup>17,19</sup> These values are significantly higher than our value of  $k_2$  and suggest a change in reaction pathway due, perhaps, to formation of  $H_2BrO_2^+$  and its reaction with  $HBrO_2$ .

The rate law establishes that one or more protons must be in the activated complex. It does not disclose, however, whether the structure of the activated complex contains only Br–O bonds as in the parent molecules or whether a Br–Br bond has formed. Interestingly, in the analogous Cl(III) disproportionation reaction,<sup>20</sup> intermediate Cl–Cl bond formation is implicated. There are some noteworthy differences between the two analogous processes. The stoichiometry and kinetics of Br(III) disproportionation are simpler than those of the much more complex Cl(III) disproportionation. At neutral and alkaline pH, the products of the latter reaction are  $Cl^-$  and  $ClO_3^-$ .<sup>20,21</sup> In acid, in the absence of initially added  $Cl^-$ , in the early stages of reaction there are three Cl-containing products;  $ClO_2$  in addition to  $Cl^-$  and  $ClO_3^-$ . In the presence of initially added  $Cl^-$ , and in later stages of reaction,

only  $\text{ClO}_2$  and  $\text{Cl}^-$  form. Thus, the greater stability of  $\text{ClO}_2$  compared with  $\text{BrO}_2$  leads to additional channels of disproportionation.

The kinetics of  $\text{Cl(III)}$  disproportionation have been studied over a wide pH range. The kinetics are much more complicated, with at least four terms identified in the rate law. At neutral and mildly acidic pH, the rate law resembles that of  $\text{Br(III)}$ , with an  $[\text{H}^+]$ -dependent term second-order in  $\text{Cl(III)}$ .<sup>22</sup> At lower pH, two additional terms appear in the rate law, because  $\text{HClO}_2$  becomes capable of oxidizing  $\text{Cl}^-$  to  $\text{HOCl}$ , giving rise to  $\text{Cl}^-$  catalysis.<sup>21</sup> The comparable process does not occur for  $\text{HBrO}_2$  in the pH range we have studied, and a similar  $\text{Br}^-$  catalysis is not observed. Lastly, an iron-catalyzed radical chain mechanism has been reported<sup>20</sup> and interpreted as evidence of reversible one-electron oxidation of  $\text{ClO}_2^-$  to  $\text{ClO}_2$  by  $\text{Fe}^{3+}$ ; a similar effect has not been observed in the  $\text{Br(III)}$  system.

**Acknowledgment.** This work was supported by Research Grant CHE-9023294 from the National Science Foundation and by Conselho Nacional de Desenvolvimento Científico e Tecnológico-CNPq (proc. 202081/90-7).

**Registry No.**  $\text{HBrO}_2$ , 37691-27-3;  $\text{BrO}_2^-$ , 7486-26-2.

#### References and Notes

(1) Systematic Design of Chemical Oscillators. 87. For part 86, see: Faria, R. B.; Lengyel, I.; Epstein, I. R.; Kustin, K. *J. Phys. Chem.* **1993**, *97*, 1164.

- (2) Faria, R. B.; Epstein, I. R.; Kustin, K. *J. Phys. Chem.* **1992**, *96*, 6861.  
 (3) Engel, P.; Oplatka, A.; Perlmutter-Hayman, B. *J. Am. Chem. Soc.* **1954**, *76*, 2010.  
 (4) Massagli, A.; Indelli, A.; Pergola, F. *Inorg. Chim. Acta* **1970**, *4*, 593.  
 (5) Faria, R. B.; Epstein, I. R.; Kustin, K. *J. Am. Chem. Soc.* **1992**, *114*, 7164.  
 (6) Hashmi, M. H.; Ayaz, A. A. *Anal. Chem.* **1963**, 908.  
 (7) Press, W. H.; Teukolsky, S. A.; Vetterling, W. T.; Flannery, B. P. *Numerical Recipes in C: the Art of Scientific Computing, 2nd ed.*; Cambridge University Press: New York, 1992. *Vide:* Coleman, F. *Minsq—Least Squares Parameter Estimation, Version 4.03*; MicroMath Scientific Software, Salt Lake City, Utah, 1991. *SlideWrite Plus Version 5.0*; Advanced Graphics Software, Inc., Carlsbad, CA, 1992.  
 (8) Jhanji, A. K.; Gould, E. S. *Int. J. Chem. Kinet.* **1991**, *23*, 229.  
 (9) Lister, M. W.; McLeod, P. E. *Can. J. Chem.* **1971**, *49*, 1987.  
 (10) Lee, C. L.; Lister, M. W. *Can. J. Chem.* **1971**, *49*, 2822.  
 (11) Cercek, B.; Ebert, M.; Keene, J. P.; Swallow, A. J. *Science* **1964**, *145*, 919.  
 (12) Soulard, M.; Bloc, F.; Hatterer, A. *J. Chem. Soc. Dalton* **1981**, 2300.  
 (13) Galal-Gorchev, H.; Morris, J. C. *Inorg. Chem.* **1965**, *4*, 899.  
 (14) Daniele, G. *Gazz. Chim. Ital.* **1990**, *90*, 1585.  
 (15) Anbar, M.; Dostrovsky, I. *J. Chem. Soc.* **1954**, 1105.  
 (16) Betts, R. H.; MacKenzie, A. G. *Can. J. Chem.* **1951**, *29*, 666.  
 (17) Ariese, F.; Ungvárai-Nagy, Z. *J. Phys. Chem.* **1986**, *90*, 1.  
 (18) Capone, S.; De Robertis, A.; De Stefano, C.; Sammartano, S.; Scarcella, R. *Talanta* **1987**, *34*, 593.  
 (19) Noszticzius, Z.; Noszticzius, E.; Schelly, Z. A. *J. Phys. Chem.* **1983**, *87*, 510.  
 (20) Kieffer, R. G.; Gordon, G. *Inorg. Chem.* **1968**, *7*, 235.  
 (21) Schmitz, G.; Rooze, H. *Can. J. Chem.* **1985**, *63*, 975.  
 (22) Kieffer, R. G.; Gordon, G. *Inorg. Chem.* **1968**, *7*, 239.